Editorial Manager(tm) for Marine Geophysical Researches
Manuscript Draft

Manuscript Number: MARI123R1

Title: THE BARAZA SLIDE. MODEL AND DYNAMICS

Article Type: SI Seafloor Mapping

Keywords: seafloor, mass flow, slide, post-mobility, geohazard, Alboran Sea

Corresponding Author: Dr David Casas, Ph.D.

Corresponding Author's Institution: Instituto Geológico y Minero de España

First Author: David Casas, Ph.D.

Order of Authors: David Casas, Ph.D.; Gemma Ercilla, Ph.d.; Mariano Yenes, Ph.D.; Ferran Estrada; Belen Alonso, Ph.D.; Margarita García, Ph.D.; Luis Somoza, Ph.D.

Abstract: The Baraza Slide is located in the northwestern Alboran Sea, between 590 and 830 m water depth, and its morphology, seismic facies and sedimentary structure are analyzed based on multibeam bathymetry and very high to medium resolution single-channel seismic records. During the Pleistocene and Late Quaternary this landslide has undergone repeated slope failures characterized by a succession of two main types of mass movement, the first of the mass-flow type and the second of the slide type. This study also reveals that the western sector of this landslide could still be active.
The relatively high slope gradients, a sedimentary column characterized by the presence of underconsolidated layers and earthquake shaking related to the active tectonic activity on the margin are the factors governing the genesis and post-mobility behavior of the Baraza mass movement. The recognition and analysis of these factors suggest that the Baraza Slide should be considered as a geo-hazard in the tectonically active Alboran Sea.

Response to Reviewers: All the corrections suggested by the reviewers have been done.
One new figure is added in order to clarify the sedimentary structure of Baraza Slide. In our opinion the figure can solve some inconsistencies indicated by the reviewers

THE BARAZA SLIDE. MODEL AND DYNAMICS

Casas, D.[1]*, Ercilla, G. [2], Yenes, M.[3], Estrada, F.[2], Alonso, B.[2], García, M.[4], Somoza, L.[1]

1 Instituto Geológico y Minero de España. C/ Ríos Rosas, nº 23. 28005 – Madrid. Spain. d.casas@igme.es +34 917287255
2 Institut de Ciències del Mar, CSIC. Passeig Marítim Barceloneta, nº 37-49. 08003-Barcelona. Spain
3 Escuela Politécnica Superior de Zamora. Universidad de Salamanca. 37008 Salamanca-Spain
4 Scott Polar Research Institute. University of Cambridge Lensfield Road, CB2 1ER Cambridge, UK

Abstract

The Baraza Slide is located in the northwestern Alboran Sea, between 590 and 830 m water depth, and its morphology, seismic facies and sedimentary structure are analyzed based on multibeam bathymetry and very high to medium resolution single-channel seismic records. During the Pleistocene and Late Quaternary this landslide has undergone repeated slope failures characterized by a succession of two main types of mass movement, the first of the mass-flow type and the second of the slide type. This study also reveals that the western sector of this landslide could still be active**.**

The relatively high slope gradients, a sedimentary column characterized by the presence of underconsolidated layers and earthquake shaking related to the active tectonic activity on the margin are the factors governing the genesis and post-mobility behavior of the Baraza mass movement. The recognition and analysis of these factors suggest that the Baraza Slide should be considered as a geo-hazard in the tectonically active Alboran Sea.

Keywords: seafloor, mass flow, slide, post-mobility, geohazard, Alboran Sea.

Introduction

Sedimentary instabilities are common features shaping the slopes of the continental margins. Our understanding of these features has increased during the last twenty years, mainly because Quaternary and subrecent events have been largely mapped and studied with high to very high resolution seismic systems, side-scan sonars and multibeam systems (Bugge et al. 1988; Masson et al. 1993; Gee et al. 2001). The combined analysis of these techniques provides excellent knowledge of the seafloor morphology and subbottom sedimentary structure, which are essential components in stability analysis (Hughes and Clarke 1996; Leroueil et al. 1996), including post-failure behavior of the sliding mass and its possible re-activation on preexisting failure planes or failed masses.

Sediment instability can be detected by the presence of slide masses, scars, or fractures (Prior 1984). It can result from a wide range of factors and processes such as erosion, sedimentation, gas, earthquakes, diapirism, glaciations and wave action (Locat and Lee, 2000; Prior 1984). To determine whether the processes responsible for the formation of mass movement on a particular slope are active, we obtained information on the geology (regional and local), detailed seafloor morphology, and rock/sediment properties.

The Baraza Slide, located in the northwestern Alboran Sea, is an example of a sedimentary instability complex in an open slope environment of a tectonically active margin. It was recently mapped between 500 and 830 m water depth (Muñoz et al. 2008) and this paper presents the first time that it is studied from a morphological and seismically point of views.

We analyze in detail the morphology of the Baraza Slide, characterize its seismic facies and define the depositional architecture model in order to establish its mechanisms of movement and evolution.

Geological Setting

The Alboran Sea is a partially land-locked, east-west–oriented basin in the westernmost Mediterranean Sea (Fig. 1), between the Spanish and Moroccan margins. The geodynamic evolution and the main structural features of the Alboran Sea result from the relative motion between Eurasia and Africa (Le Pichon et al. 1971; Olivet et al. 1973; Ryan et al. 1973; Dewey et al. 1989; Comas et al. 1992; Maldonado et al. 1992; Docherty 1993; Watts et al. 1993). Post-Tortonian tectonics modified the architecture of the Miocene basins and margins, forming the present structure, seafloor morphology and structural boundaries of the Alboran Sea (Comas et al. 1992).

The Alboran Sea displays a complex physiography, with several basins separated by structural highs (Olivet et al. 1973; Dewey et al. 1989). During the Quaternary the Alboran margin to developed a variety of sedimentary growth patterns due to the interplay of tectonism, glacio-eustatic sea-level changes, and a variable marine circulation system. These are characterized mostly by shelf-margin deltas on the proximal margin and on the distal margins and in the basin areas by mass-movements, turbidite systems and contourites (Huang and Stanley 1972; Ammar 1987; Tesson et al. 1987; Baraza et al. 1992; Ercilla et al. 1992; Ercilla et al. 1994; Estrada et al. 1997; Ercilla et al. 2002; Alonso and Ercilla 2007, among others). The sedimentary mass-movement systems are mostly associated with structural highs, turbidite systems and locally, as in the Baraza Slide, with open slope deposits. The studied sector of the open slope has thus been characterized by the occurrence of mass-movement events during the Quaternary and particularly during the Pliocene, when mega-slides were deposited (Ercilla et al. 1992; Baraza et al. 1992; Pérez-Belzuz 1999).

Regional studies of the seismicity of the Alboran Basin indicate that earthquakes are numerous and extend over the entire Spanish margin (Udías et al. 1976; Sanz de Galdeano and López 1988). Earthquake magnitudes are moderate in general, but there is historical and recent evidence of strong earthquakes in the area (Udías et al. 1976). Although a typical earthquake within the area has a magnitude of < 4, earthquakes with a magnitude of 7.0 may occur offshore near the western Alboran Sea slope (Hatzfeld 1976; Udías et al. 1976). The epicenters in the western Alboran Sea are linked to the main tectonic features (International Seismological Centre: http://www.isc.ac.uk). Moreover, geotechnical studies carried out on the Malaga slope, close to the study area, indicate that the western Alboran Sea slope is characterized as potentially unstable (Baraza et al. 1992).

Geophysical Data

The data used to study the Baraza Slide were obtained by multibeam bathymetry and single-channel seismic profiles collected during several cruises (SAGAS, SAGASBIS, GC90-1). The seafloor multibeam bathymetry provided by the *Ministerio de Medio Ambiente y Medio Rural y Marino (Secretaria General del Mar)* was obtained using a Simrad EM12 multibeam echosounder. A total of 11 single-channel seismic profiles were studied (Fig. 2), including 8 very high resolution TOPAS (TOpographic PArametric Sonar) profiles, 1 high resolution Sparker profile (from http://www.igme.es/internet/sistemas_infor), and 2 medium resolution airgun profile (sleeve guns, 120 c.i.). The penetration of the acoustic signal achieved with the TOPAS system varies between 30 and 200 milliseconds

(twtt) at full oceanic depths and the resolution is decimetric. The penetration of the Sparker acoustic signal is about 1.5 s (twtt) and it provides a metric resolution, while the penetration of the airgun signal is about 2-3 s (twtt) and it provides a resolution of tens of meters.

Kingdom suite software was used to analyze and interpret the seismic profiles.

Results

Morphology

The Baraza Slide is located between 590 and 830 m water depth in the slope province of the northwestern Alboran Sea (Fig. 3). The gradients are between 2º and 3.5º (Fig. 4), becoming smoother downslope with a gradient of < 1.5º below 750 m water depth. This smooth, gentle surface dips toward the south and extends down to 900 m water depth (Figs. 3 and 4). Apart from the Baraza Slide, other morphological features are present on the slope: structural features (highs and fault scarps), fluid-dynamic features, channels and canyons (Fig. 3).

Three structural highs (Algarrobo Bank at 780 water depth, Herradura Norte Bank at 800 m water depth, and an unnamed one at 900 m water depth) are located 24 km (to the SW), 30 km (to the SE) and 32 km (to the ESE) respectively from the Baraza Slide (Fig. 3). They display subrounded and trapezoidal shapes with a maximum diameter of 10, 5 and 3 km, respectively (Fig. 3), and have a relief of 350, 250 and 140 m, respectively.

A complex of SSW-NNE faults is observed between the Algarrobo and Herradura Norte Banks. Also, SSW-NNE and NNW-SSE faults are observed about 20 km to the ESE of the Baraza Slide (Fig. 3). These faults produce linear seafloor irregularities a few km to ≈ 20 km in length and a few meters in relief.

Several fluid-dynamic features are observed 18 km to the WSW from the Baraza Slide. At least 4 pockmarks can be differentiated. Topographically, they have U-shaped cross-sections and average dimensions of 400 m diameter and < 25 m relief.

Canyons and channels are concentrated to the east of the Baraza Slide. They form two complexes that extend from the shelf edge down to the slope: the western complex to about 600 m water depth and the eastern complex to about 900 m water depth (Fig. 3). The eastern complex represents the Calahonda and Sacratif Turbidite systems (Pérez-Belzuz 1999). These complexes are formed by channels and canyons that evolve to channels, display U- and V-shaped cross-sections, and have sinuous to rectilinear pathways in plain view. Their dimensions are variable, with lengths ranging from 2 to 19 km, widths of hundreds of meters, and reliefs ranging from < 15 to 180 m.

Morphology of the Baraza Slide

The Baraza Slide is an isolated mass-movement feature. Its plan-view morphology is clearly defined by the presence of a well-developed headwall associated downslope with a striking rough seafloor area (Figs. 4 and 5).

The headwall, located between 590 and 600 m water depth, is expressed as a seafloor scarp with higher gradient (5º) than the surrounding slope (2º to 3.5º). This feature, with a total length of about 14.6 km is expressed as a concave downslope depression with an irregular scoop shape. The headwall is constituted by at least two smaller scars (hereinafter named H1 and H2, from western to eastern) that represent individual, smaller-scale headwalls (Fig. 5). Scar H1 has a length of about 9.7 km, a maximum incision of 53 m and an average gradient of 5º. Scar H2 is smaller, with a length of about 4.9 km, an average relief of < 30 m and a maximum gradient of 3º (Fig. 4).

Further downslope of the headwall, between 600 and 830 m water depth, there is a rough seafloor area of about 116 km^2, where it is possible to identify two domains displaying variations in surface roughness, one more pronounced than the other, and both with an irregular lobe shape (hereinafter named lobes A and B). Lobe A, which displays the roughest seafloor, is located on the western side, extending from H1 down to 770 m water depth; it is the smaller of the two (7.6 km long) and has two finely distinct toes. Lobe B extends from H2 down to 830 m water depth; it is 9.7 km long, and surrounds lobe A showing two striking toes (Fig. 5).

Sedimentary Structure and Seismic Facies

The main elements characterizing the sedimentary structure of the Baraza Slide are the following: a) a slide scar, b) mass-flow deposits, and c) the overlying post-mass-flow sediments.

The acoustic character of the slide scar varies laterally. It is a highly reflective, erosive seafloor surface that truncates the stratified slope deposits at H1 (Fig. 6). In contrast, H2 is buried by about 30 ms of stratified slope sediments. The scar plane extends downslope, going into subsurface sediments and joining with the basal scar plane, i.e. the shear plane (Fig. 6), which is overlaid by mass-flow sediments and their overlying sediments. This irregular, erosive surface (relief erosion down to 15 ms) is parallel to the stratification and toward the flanks of the deformed sediments it is a planar surface that seems to show no evidence of erosion (Fig. 7).

The mass-flow deposits display different seismic facies according to the type of seismic records. The medium (airgun) and high (sparker) resolution seismic profiles show a mounded geometry (11.8 km long) with a wedge shape in longitudinal section and a lenticular shape in oblique cross-section (Fig. 6). The maximum thickness of this wedge is about 40 ms. The upper surface of the depositional body displays a gradual downslope change from a pronounced upward convexity to a slight convexity and/or practically flat lying sections at its periphery. It is acoustically defined by discontinuous irregular reflections that can be correlated laterally, although locally not discernible at all (Fig. 6). Internally, the mass-flow deposit is mostly defined by chaotic facies that laterally change to transparent facies toward the flanks and toe. The width of the area affected by this transparent facies is distributed as a peripheral fringe that varies in width from 600 m on the western side to 2.1 km at the distal toe. Within the transparent facies (about 20 ms thick) at least two stacked transparent levels are differentiated, each 10 ms thick (Fig. 7). The lower boundary of this wedge is observed exclusively on the airgun and sparker profiles, and is an irregular concave-upward surface (ten ms in relief) with an erosive character (Fig. 7), indicating the incorporation of underlying sediments during its emplacement.

In the TOPAS profiles, the mass-flow deposits show mostly transparent facies (Fig. 8). These records do not image the lower boundary of the deposit but its upper boundary shows a great variety of acoustic features. In fact, the uppermost part of the mass-flow deposit is a highly deformed level about 10 ms thick, formed by discontinuous, contorted reflections, isolated hyperbolas, and outflowing acoustic features that will be described in the following section. This deformed level is identified throughout the mass-flow sediments, except at the foot of the slide scar, where the uppermost part has a planar configuration (Fig. 8). The upper surface of the mass-flow deposits generally display a similar slope to that of the seafloor, with gradients decreasing downslope (2.5º to 1º), except for the profiles located away from the H1. Here, the slope profile of the upper surface shows breaks of slope, changing downslope from lower to higher gradients and again to lower ones.

The high degree of deformation of the upper surface, the erosive character of the lower boundary, and the transparent-to-chaotic seismic facies were the criteria used to define this deposit as a mass-flow (Hampton et al. 1996; Posamentier 2003).

The rough topography produced by mass flow deposits is subdued by the overlying sediments, which we have defined as post-mass-flow sediments. These sediments are acoustically defined by the alternation of stratified facies of high and low amplitudes, mostly with a seaward-divergent configuration. These facies form a level whose thickness varies downslope: from 80 to 25-30 ms when the post-mass flow unit is truncated by H1, and from 30 to 80 ms when it covers H2. The post–mass-flow sediments are affected by outflowing and strata deformational features (Fig. 8).

Outflowing and Deformational Features

The outflowing features are intrusive fluid flow structures acoustically characterized by transparent diapir-like features affected by contorted, dome-shaped reflections, loss of stratification, diffractions, and isolated echoes (Fig. 8). Large- and small-scale fluid flow features are identified. The large-scale ones occur mostly over the deformed chaotic sediments and show the trend to decrease in size downslope. The small-scale ones occur in the perimeter domain of the mass-flow deposits, where the transparent facies are mapped. The immediately overlying sediments (i.e. those of the post-mass-flow deposits) display convex-upward seismic layers, whose curvature lengths are proportional to the scale of the fluid flow structures (100 m maximum). Likewise, the thickness of the affected overlying sediments varies between 40 ms for the large scale ones to 10 ms for the small-scale ones.

Deformation affects the strata configuration and lateral continuity of the overlying post-mass-flow sediments, and is well developed in the sediments downslope from H1. The deformational features include folds and faults. Two gentle anticline features (wavelength about 3 km) are identified. Their hinges produce breaks of slope of the seafloor, and the upslope flanks are gentler than the downslope ones (Fig. 8). Subtle lateral thickening and thinning (a few milliseconds) of the individual layers is observed, being more evident at the foot of the slide scar.

High-angle faults offsetting the post-mass-flow sediments are also identified. They comprise reverse and normal faults (Fig. 8). Densely distributed faults are associated with the fluid flow features, and some of them, mostly the reverse faults, also with the hinges of the anticlines. Reverse faults have a plane dipping toward the north with a maximum displacement of 10 ms and propagating over 20 ms through the post-mass-flow sediments. The faults with a normal displacement (3 ms in average) are characterized by subvertical planes and occur mostly close to H1 (Fig. 8). The thickness of the sediments affected by these faults varies between 10 and 25 ms.

Age Control from Seismic Data

We have considered the Quaternary deposits as the “background unit” within which the Baraza Slide developed. To estimate their age based on seismic data, we compared and correlated the Quaternary slope deposits of

the studied sector with seismic divisions and their bounding discontinuity ages defined in equivalent sedimentary records from other margin slopes around Iberia (Ercilla et al. 1994, 2002, 2008; Hernández-Molina et al. 2002; Llave et al. 2001, 2006, 2007; Hernández-Molina et al. 2002, 2006: Stow et al. 2002; García et al. 2006). The isochronic stratigraphic framework defined by these records is based on considerations of eustatic sea level and climatic and paleoceanographic changes (Shackleton 1987; Alonso and Maldonado 1992; Ercilla et al. 1994; Revel et al. 1996; Zazo 1999; Zachos et al. 2001; Waelbroeck et al. 2002; Head and Gibbard 2005; Lisiecki and Raymo 2005, 2007).

Comparison and correlation of the background deposits with the Quaternary deposits in different areas has been mostly based on seismic characters, such as amplitude, continuity and reflection configuration, vertical trending of reflections, and type of boundary between levels of similar facies. Within the "background unit" three chronostratigraphic boundaries represented by reflectors A, B and C, from top to bottom, were defined (Fig. 7). These reflectors are characterized by their high acoustic amplitude and lateral continuity, mark sharp changes in the acoustic facies of the bounding deposits, and locally can display an erosive character; all of these characteristics together make these reflectors easily traceable throughout the studied slope. In the other slopes around Iberia and presumably in this one as well, reflector C corresponds to the MPR (Middle Pleistocene Revolution) discontinuity (MIS 22/21; 0.9/0.92 Ma); reflector B is associated with the boundary between the isotopic stages MIS 18/17 (0.69 Ma); and reflector A corresponds to the LGM (Last Glacial Maximum) discontinuity (MIS 2/1; 24 ka).

These seismic boundaries divide the background deposits into three seismic units, I, II and III, from younger to older (Fig 7 and 8). Within this stratigraphic framework, the mass-flow deposit occurs in seismic unit II, showing how the lower boundary of the chaotic facies erodes the underlying seismic unit III and that of the transparent facies rests on boundary B. The post-mass-flow deposits correspond to deposits of the upper part of units II and III. Likewise, it is observed that the shear plane affects deposits of the upper part of seismic units I and II, especially in front of H1 (Fig 6, 7 and 8). All these observations show that the mass flow likely began to develop just after 690 ka but the development of the shear plane either continued during the emplacement and deposition of post-mass-flow deposits or formed recently, affecting these deposits. We cannot give more precise details but we can suggest that at least in the area related to H1, the mass flow was active after the LGM and that its dynamics is subactual.

Discussion

Formation Model and Dynamics

The sediment dynamics and evolution of the Baraza Slide can be interpreted on the basis of its well-defined morphology, geometry, and internal pattern and the vertical trend of the seismic facies, features and surfaces. It is interesting to study all these elements together since they tend to preserve depositional or stopping structures and can yield valuable information on dynamic landslide emplacement (Masson et al. 1993). The proposed model for the genesis and development of the Baraza mass movement is represented here as comprising three stages: metastable, flowing and sliding (Fig. 9).

Before 690 Ka, the NW Alboran slope was in metastable equilibrium, mainly governed by downslope gravitational forces. The slope condition was favored by the interplay of morphologic, sedimentary and seismic factors. This slope shows the steepest gradients (3º to 3.5º) of the open regional slope, and under this gravitational equilibrium the bedding planes defined by vertical stacking of the lower Quaternary stratified deposits may have acted as a layer or zone of weakness. This is suggested because the subsequent shear plane is subparallel to older strata and is roughly parallel to the regional slope.

The *flowing stage* began when the metastable equilibrium was broken, perhaps during an earthquake, some time just after 690 ka. This stage occurred when the downslope-oriented shear stress exceeded the shear strength, resulting in the development of an instability plane within the stratified slope deposits (Fig. 9). This new situation created two main sediment packages separated by a discontinuity surface (i.e. failure plane) subparallel to the stratification. It is a concave-upward irregular surface with an erosive character (Fig. 7).The flowing stage implies a translational displacement of the main body of the Baraza Slide along the failure plane. In this stage, the scar, which corresponds to the H1and H2, was formed while the displaced mass moved and evolved into a non-Newtonian flow, as is inferred from the chaotic facies that characterize the final deposit. During the downslope movement, the mass flow seems to have been affected by a progressive dilution of the flow concentration as suggested by the change in acoustic facies, from chaotic to transparent (Fig. 7).

The erosive character of the basal surface of the mass-flow deposits during this stage appears to have mobilized material from the underlying seismic unit III deposits (Fig. 7). The ability of submarine sediment failures to substantially erode the substrate has been previously demonstrated and has important implications as it allows a flow to increase in volume, and therefore to gain run-out potential (Gee et al. 1999). However, in the Baraza Slide (a

few km long) no long run-out occurred, probably because of a sharp decrease in slope gradients, from 3.5º to 0.5-1º, favoring an increase in resistance to the flowing process, which would freeze and thus stop the mass-flow.

During this stage, the mass flow either involved two different flowing events or one event affecting a larger area in the east decreasing to a smaller area in the west. In fact, with our seismic data it was possible to differentiate the occurrence of two different mass-flow events within the Baraza mass-flow deposits. This fact is also supported by the different seafloor roughness of mapped lobes A and B on the multibeam bathymetry which are outlining the area affected by the Baraza mass-flow deposits. These lobes could be a morphology related to a sub-superficial expression of the Baraza deposits. We are aware that our seismic data do not allow us to associate sedimentary mass-flow units with lobes A and B. For this reason in this study the term "lobe" is used in a morphological sense.

The *sliding stage* occurred when the Baraza Slide was reactivated with a different instability mechanism: a slide-type movement. This movement affected both the buried mass-flow deposits and the overlying sediments, which moved with a shear-dominated movement along the plane of the scar (Fig. 9). This is confirmed by the lateral continuity of the scar with the basal boundary of the mass-flow deposits and the formation of structural and outflowing features due to the stress caused by the shearing movement. The presence of two slide scars, H1 and H2, suggests a decrease in the active area of the sliding from west to east (Fig. 8). The fact that not only the reflector A (LGM) but also the most recent sediment (seafloor reflector) are truncated by H1 reveal that the sliding stage is relatively recent in this sector and that is during this stage when the H1 is formed representing a reactivation of a portion of the main scarp. This evidence leads us to think that the sliding stage became effective especially in the western sector of the Baraza Slide and that its dynamics is subactual (Fig. 9). An alternative hypothesis to explain the presence of lobe A, which appears to be a more recent morphology than lobe B, arises from the sliding movement. Due to its size and position in front of H1 (Fig. 5) is reasonable to think that lobe A is a superficial morphology resulting from the deformation associated to sliding movement.

The sliding model combines extensional and compressional deformation. The extensional domain is located in the slide scar area, where tensional failure is observed, and at the foot of the scar, where the post-mass-flow sediments are unaffected by outflowing features. The compressional deformation produced by the slide evolution is revealed by the formation of the two anticlines and outflowing features, and their particular size distribution. Regarding the outflowing features, although no long run-outs characterize the Baraza mass flow, the motion of the slide can produce favorable conditions for generating water escape structures from the water entrained during sediment flow (De Blasio et al. 2005).

Triggering Mechanism

A triggering mechanism, or a combination of triggering mechanisms, is required to destabilize sediments already prone to failure. In the case of the Baraza Slide the exact triggering mechanism is unclear, although we tentatively suggest that the landslide was probably initiated by the following combination of mechanisms. The relatively high slope gradients (2º to 3.5º) and the rapid deposition of sediments directly onto the slope during the high amplitude lowstand stages were probably the main predisposition factors, however, failure could have been triggered by seismic shaking (or by tectonic-related activity). The potential link between high slope gradients, underconsolidation, earthquakes and instability along continental margins has been discussed by numerous authors (Hampton et al. 1996; Mulder and Cochonat 1996; among others).

The chronostratigraphic correlation (Fig. 6) indicates that the onset of the Baraza Slide took place after the Middle Pleistocene Revolution, specifically just after 0.69 Ma (isotopic stage boundary MIS 18/17). After the MPR, the high frequency sea-level changes tend to be of higher amplitudes (Ercilla et al. 1992; Iglesias 2009) and on the Spanish margin of the Alboran Sea lowstands favored the sediment supply directly to the slope (Ercilla et al. 1992; 1994). Likewise, the asymmetric character of those changes (falling 65% of the time, Chiocci et al. 1997) suggests that the Alboran margin is in fact the result of the vertical stacking of lowstand deposits that on the open slope tend to be bounded by conformity surfaces that represent erosive and/or condensed polygenetic surfaces (Ercilla et al. 1994; Perez-Belzuz 1999). During the isotopic stage boundary MIS 18/17, a global glacio-eustatic fall also occurred, and in the Alboran Sea it produced coast line migration through the narrow shelf, reaching the shelf break or even below it, with high sedimentation rates from the hinterland sources. The high sedimentation rate implies underconsolidation of the sedimentary column and consequent degradation of the sediment shear strength (Hampton et al. 1996; Larberg and Vorren 2000). Under this slope condition, bedding planes may act as layers or zones of weakness. In the case of the Baraza Slide, similar environmental conditions are suggested, because the shear plane is formed by a layer subparallel to older strata (Fig. 6).

With respect to seismicity as a triggering mechanism, the geological framework of the Alboran Sea is also characterized by its tectonic activity, as is indicated by the strong earthquakes (up to magnitude 7) that have occurred in the study area (Hatzfeld 1976; Udías et al. 1976; Sanz de Galdeano and López 1988). Earthquake shaking could

therefore be the main triggering mechanism of the Baraza Slide. The proximity of the slide to the SSW-NNE and NNE-SSW faults and the Algarrobo and Herradura Norte Banks, which are volcanic in origin (Ballesteros et al. 2008; Pérez-Belzuz 1999), allow us to consider these features as potential geological structures that generate earthquakes and therefore trigger slope failures (Fig. 3). Another observation that supports this hypothesis is the great amount of ancient mass-flow deposits, with different orders of magnitude, recorded in the upper Pliocene and lower Quaternary slope deposits of the study area (Baraza et al. 1992; 1994; Ercilla et al. 1994; Perez-Belzuz 1999) (Fig. 7). This fact reinforces the idea that open slope conditions, with relatively high gradients and an underconsolidated sediment condition configure a slope ready for failure; however, the energy provided by earthquake shaking is usually required as a trigger.

Following the approach taken by Baraza et al. (1994) who estimate the seismic stability of the western Alboran Sea slope, an average distance of 13 km is required for a 7.0 magnitude earthquake to induce a horizontal ground acceleration of 0.43 g, sufficient to produce a surficial slope failure. A 7.0 magnitude earthquake may induce a ground acceleration of 0.16 g, necessary to initiate a failure at 25 m depth, at a distance of 33 km from the seismic source. The effects of an earthquake of a given magnitude may be amplified by the local soil conditions, and the distance to which these acceleration values are induced may therefore be higher (Baraza et al. 1992; 1994). The existence of potential seismogenic structures within a 13-33 km area from the Baraza Slide is consistent with the seismic trigger hypothesis.

All these factors are valid for the flowing and sliding stages defined. Before the sliding stage started, the slope maintained a configuration defined by fairly high gradients and underconsolidated sediments. The mechanism of deposition for the mass-flow-type movement implies a sudden emplacement of the high porosity displaced mass that would be the same as the deposition of a thick underconsolidated unit. This deposit can develop high pore pressure due to the overburden associated with the overlying post-mass-flow sediments and consequently may act as a layer or zone of weakness (equivalent to the metastable stage configuration defined above) during the sliding stage. This "weak" sedimentary column configuration could explain the reactivation and post-mobility behavior of the Baraza Slide in response to an external trigger such as an earthquake.

Conclusions

The Baraza Slide is an example of a landslide imaged by very high resolution multibeam and seismic systems. Its recognition and analysis suggest that it is a geo-hazard in the tectonically active Alboran Sea.

The combined results obtained from the morphology and seismic analysis indicate that the Baraza landslide is a Pleistocene (0.69 Ma) sedimentary instability complex that has undergone repeated slope failures. The proposed model for the genesis and development of the Baraza mass movement is represented by three stages, metastable, flowing and sliding, which represent a simple scenario for describing a complex formed by a mass-flow that changes to a slide system over time. This study also reveals that the western sector of this landslide could still remain active.

The relatively high slope gradients and rapid deposition of sediments directly onto the continental slope during sea level falls and lowstand stages were probably the main conditioning factors destabilizing the slope. The proximity of the landslide to probable earthquake epicenters related to active tectonic features could also be a key factor governing the triggering of the Baraza Slide. The deposition of high porosity mass-flow sediments as an underconsolidated unit that can develop high pore pressures seems to be the most likely predisposition factor for explaining the reactivation and the post-mobility behavior of the gravity processes observed in the slide during the Late Quaternary.

Acknowledgement

This article is dedicated to Dr. Jesus Baraza. This study was supported by the Projects SAGAS (CTM2009/07893-E/MAR and CTM2005-08071-C03-02/MAR), CONTOURIBER (CTM2008-06399-C04-04/MAR) and MONTERA (CTM2009-14157-C02), of the Spanish Ministry of Education and Science. The Continental Margins Group (GMC) also thanks the *Generalitat de Catalunya* for the financial support received in the framework of 2009 SGR1071. We thank Seismic Micro-Technology Inc. for supporting us with the Kingdom Suite Program. We also, thank to Ministerio *de Medio Ambiente y Medio Rural y Marino (Secretaria General del Mar)* for the bathymetric data. The helpful comments from the reviewers are gratefully acknowledged.

References

Alonso B, Maldonado A (1992). Plio-Quaternary margin growth patterns in a complex tectonic setting (Northeastern Alboran Sea). Geo-Mar Lett 12(2/3): 137-143.

Alonso B, Ercilla G (2007). Small turbidite systems in a complex tectonic setting (SW Mediterranean Sea): morphology and growth patterns. Mar Petrol Geol 19: 1225-1240.

Ammar A (1987). Analyse sismique des corps sédimentaires quaternaires de la marge méridionale de la mer d'Alboran. These 3ème cycle, Univ. Perpignan, 150 pp.

Ballesteros M, Rivera J, Muñoz A, Muñoz-Martín A, Acosta J, Carbó A, Uchup E (2008). Alboran Basin, southern Spain—Part II: Neogene tectonic implications for the orogenic float model. Mar Petrol Geol (25-1):75-101 .

Baraza J, Ercilla G, Lee H (1992). Geotechnical properties and preliminary assessment of sediment stability on the continental slope of the Northwestern Alboran Sea. Geo-Mar Lett 12: 150-156.

Baraza J, Ercilla G (1994). Geotechnical properties of near-surface sediments from the Northwestern Alboran Sea Slope (SW Mediterranean): Influence of texture and sedimentary processes. Mar Georesour Geotec 12: 181-200.

Bugge T, Belderson R.H, Kenyon N.H (1988). The Storegga slide. Philos. Trans. R. S. London 325: 357–388.

Chiocci F. L, Ercilla G, et al. (1997). Stratal architecture of Western Mediterranean Margins as the result of the stacking of Quaternary lowstand deposits bellow "glacio-eustatic fluctuation base-level. Sed Geol 112: 195-217.

Comas M.C, García-Dueñas V, Jurado M.J (1992). Neogene tectonic evolution of the Alboran Sea from MCS data. In: The Alboran Sea. Special Issue (A. Maldonado ed.), Geo-Mar Lett 12: 157–164.

De Blasio F. V, Elverhoi A, et al. (2005). "On the dynamics of subaqueous clay rich gravity mass flows - the giant Storegga slide, Norway." Mar Petrol Geol 22(1-2): 179-186

Dewey J.F, Helman M.L, Turco E, Hutton D.H.W, Knott S.D (1989). Kinematics of the Western Mediterranean, J. Geol. Soc London Sp Publ 45: 265-283.

Docherty J.I.C, (1993). Subsidence and Tectonics of the Alboran Sea Basin, Western Mediterranean. Ph.D., Univ. de Barcelona, Barcelona, 185 pp.

Ercilla G, Alonso B, Baraza, J (1992). Sedimentary Evolution of the Northwestern Alboran Sea during the Quaternary. Geo-Mar Lett 12: 144-149.

Ercilla G, Farran M, Alonso B, Díaz JI (1994). Pleistocene progradational growth-pattern of the northern Catalonia continental-shelf (northwestern Mediterranean. Geo-Mar. Lett. 14(4): 264-271.

Ercilla G, Baraza J, Alonso B, Estrada F, Casas D, Farran M (2002). The Ceuta Drift, Alboran Sea, southwestern Mediterranean. In: Deep-Water Contourite Systems: Modern Drifts and Ancient Series, Seismic and Sedimentary Characteristics. Stow D.A.V., Pudsey C.J., Howe J.A., Faugères J.-C., Viana A.R. (Eds). Geol. Soc. London Memoirs 22: 155-170.

Ercilla G, Casas D, Estrada F, Vázquez J.T, Iglesias J, García M, Gómez M, Acosta J, Gallart J, Maestro A, Marconi Team (2008). Morphosedimentary features and recent depositional architectural model of the Cantabrian continental margin. Mar. Geol 247: 61-83.

Estrada F, Ercilla G, Alonso B (1997). Plio-Quaternary tectosedimentary evolution of the northeastern Alboran Sea. Tectonophysics 282: 423-442.

García M, Alonso B, Ercilla G, Gràcia E (2006). The Tributary Valley Systems of the Almeria Canyon (Alboran Sea, SW Mediterranean): Sedimentary Architecture. Mar Geol 226: 207-223.

Gee M.J.R, Masson D.G, Watts A.B, Allen P (2001). Passage of debris flows and turbidity currents through a topographic constriction: seafloor erosion and deflection of pathways. Sedimentology 8: 1389–1411.

Hampton M.A, Lee H.J, Locat J (1996). Submarine landslides. Rev Geophys 34:33–59.

Hatzfeld D (1976). Étude de sismicité dans la region de l'Arc de Gibraltar. Annales Geophysicae 32:71-85.

Head M.J, Gibbard P.L (2005). Early-Middle Pleistocene transitions: an overview and recommendation for the defining boundary. In: Early-Middle Pleistocene Transitions: The Land-Ocean Evidence. Head, M.J. & Gibbard, P.L. (Eds). Geol. Soc. London Sp Publ 247: 1-18.

Hernández-Molina FJ, Somoza L, Vázquez JT, Lobo FJ, Fernández-Puga MC, Llave E, Díaz del Río V (2002). Quaternary stratigraphic stacking patterns on the continental shelves of the southern Iberian Peninsula:Their relationship with global climate and palaeoceanographic changes. Quatern Int 92, 1: 5-23

Hernández-Molina F.J, Llave E, Stow D.A.V, García M, Somoza L, Vázquez J.T, Lobo F.J, Maestro A, Díaz del Río V, León R, Medialdea T, Gardner J (2006). The contourite depositional system of the Gulf of Cadiz: A sedimentary model related to the bottom current activity of the Mediterranean outflow water and its interaction with the continental margin. Deep-Sea Res. Pt II, 53(11-13): 1420-1463.

Hughes Clarke JE, Mayer LA, Wells D.E (1996). Shallow-water imaging multibeam sonars: A new tool for investigation seafloor processes in the coastal zone and on the continental shelf. Mar. Geophys Res 18: 607-629.

Huang T. C, Stanley D. J (1972). Western Alboran Sea: Sediment Dispersal, Ponding and Reversal of Currents. The Mediterranean Sea: a Natural Sedimentation Laboratory. Stroudsbourg, P.A., Dowden, Hutchinson and Ross**,** 521-559 pp.

Iglesias J (2009). Sedimentation on the Cantabrian Continental Margin from Late Oligocene to Quaternary. Ph.D. Thesis. ICM-CSIC & Univ. of Vigo.

Laberg J.S, Vorren T.O (2000). The Trandjupet slide, offshore Norway-morphology, evacuation and triggering mechanisms. Mar Geol 171 (1-4): 95–114.

Le Pichon X, Bonnin J, Francheteau J, Sibuet J.C (1971). Une hypothèse tectonique du Golfe de Gascogne. In: Histoire Structurale du Golfe de Gascogne. Debysier J., Le Pichon X, Montadert L (Eds.). Publication de l'Institute Français du Pétrole, Technip, Paris, p. VI.11.1 - VI.11.44

Leroueil S, Vaunat J, Picarelli L, Locat J, Lee H, Faure R (1996). Geotechnical characterization of slope movements. Proceedings of the 7th International Symposium on Landslides, Trondheim. 1: 53-74.

Lisiecki L.E, Raymo M.E (2005). A Pliocene-Pleistocene stack of 57 globally distributed benthic d18O records. Paleoceanography 20(2): 1-17

Lisiecki L.E, Raymo M.E (2007). Plio-Pleistocene climate evolution: trends and transitions in glacial cycle dynamics. Quaternary Sci Rev 26(1-2): 56-69.

Llave E, Hernández-Molina F.J, Somoza L, Díaz-del Rio V, Stow D.A.V, Maestro A, Alveirinho Dias J.M (2001). Seismic stacking pattern of the Faro-Albufeira contourite system (Gulf of Cadiz): a Quaternary record of paleoceanographic and tectonic influences. Mar Geophys Res 22: 487-508

Llave E, Schönfeld J, Hernández-Molina F.J, Mulder T, Somoza L, Diaz-del Rio V, Sanchez-Almazo I (2006). High-resolution stratigraphy of the Mediterranean outflow contourite system in the Gulf of Cadiz during the late

Pleistocene: The impact of Heinrich events. Mar Geol 277: 241-262.

Llave E, Hernández-Molina F.J, Somoza L, Stow D.A.V, Díaz del Río V (2007). Quaternary evolution of the contourite depositional system in the Gulf of Cadiz. In: Economic and Palaeoceanographic Significance of Contourite Deposits. Viana A.R, Rebesco M (Eds.). Geol. Soc. London Spec Publ 276: 49-79.

Locat J, Lee H (2000). Submarine landslides: Advances and challenges. Proceedings of the 8th International Symposium on Landslides, Cardiff.

Maldonado A, Campillo A.C, Mauffret A, Alonso B, Woodside J, Campos J (1992). Alboran Sea late Cenozoic tectonic and stratigraphic evolution. In: Maldonado, A. (Ed.), The Alboran Sea. Geo-Mar Lett 12 (2/3): 179-186.

Masson D.G, Huggett Q.J, Brunsden N (1993). The surface texture of the Saharan debris flow deposit and some speculations on submarine debris flow processes. Sedimentology 40: 583-598.

Mulder T, Cochonat P (1996). Classification of offshore mass movements. J Sediment Res 66: 43– 57.

Muñoz A, Ballesteros M, Montoya I, Rivera J, Acosta J, Uchupi E (2008). Alboran Basin, southern Spain—Part I: Geomorphology. Mar Petrol Geol (25): 59-73.

Olivet, J.L, Pautot, G, Auzende, J.M (1973). Structural framework of selected regions of the Western Mediterranean: Alboran Sea. Init Rep DSDP 13: 1417-1430.

Pérez-Belzuz F (1999). Geología del Margen y Cuenca del Mar de Alborán Durante el Plio-Cuaternario: Sedimentación y Tectónica. PhD Thesis, Univ. of Barcelona (UB), 538 pp.

Posamentier H.W, Kolla V (2003). Seismic geomorphology and stratigraphy of depositional elements in deep-water settings. J Sediment Res 73: 367– 388.

Prior D.B (1984). Submarine landslides. In: Proceedings of the 4th International Symposium on Landslides, Toronto, 2: 179-196

Revel M, Crémer M, Grousset F.E, Labeyrie L (1996). Grain-size and Sr-Nd isotopes as tracer of paleo-bottom current strength, Northeast Atlantic Ocean. Mar Geol 131: 233-249.

Ryan W.B.E. Hs, Cita M.B, Dumitricia E, Lort, J, Maync W, Nesteroff W.D, Pautot G, Stradner H., Wezel, F.C (1973). Western Alboran Basin Site-121. Init Rep DSDP 13: 43-89.

Sanz de Galdeano C, López Casado C (1988). Fuentes sísmicas en el ámbito bético-rifeño. Revista de Geofísica 44:175-198

Shackleton N.J (1987). Oxygen Isotopes, Ice Volume and Sea-Level. Quaternary Sci. Rev 6(3-4): 183-190

Stow D.A.V, Faugères J.C, Howe J.A, Pudsey C.J, Viana A.R (2002). Bottom currents, contourites and deep-sea sediment drifts: current state-of-the-art. In: Deep-Water Contourite Systems: Modern Drifts and Ancient Series, Seismic and Sedimentary Characteristics. Stow D.A.V., Pudsey C.J, Howe J.A, Faugères J.C, Viana A.R (Eds). Geol Soc London Memoirs 22: 7-20

Tesson M, Gensous B, Lambraimi M (1987). Seismic analysis of the southern margin of the Alboran Sea. Journal of African Earth Sciences 6: 813-821.

Udías A, Lopez Arroyo A, Mezcua J (1976). Seismotectonic of the Azores Alboran region. Tectonophysics 31:259-289.

Waelbroeck C, Labeyrie L, Michel E, Duplessy J. C, McManus J. F, Lambeck K. Balbon E, Labracherie M (2002). Sea-level and deep water temperature changes derived from benthic foraminifera isotopic records. Quaternary Sci Rev 21 (1-3): 295-305.

Watts A.B, Platt J.E, Buhl E (1993). Tectonic evolution of the Alboran Sea basin. Basin Reses. 5: 153-177.

Zachos J, Pagani M, Sloan L, Thomas E, Billups K (2001). Trends, rhythms, and aberrations in global climate 65 Ma to present. Science 292(5517): 686-693.

Zazo C (1999). Interglacial sea levels. Quatern Int 55: 101-113.

Figures

Fig. 1 Bathymetry of the Alboran Sea in the westernmost Mediterranean Sea and detailed study area. The seafloor multibeam bathymetry, mapped using a Simrad EM12 multibeam echosounder, was provided by the Ministerio de Medio Ambiente y Medio Rural y Marino *(SPACE PROJECT).*

Fig. 2 Location of the geophysical data set available in the study area. Red lines represent the TOPAS profiles, black lines represent the sparker profile, and pink lines represent the air-gun seismic profile. The location of Figures 6 and 7 is also displayed.

Fig. 3 Map showing the physiography of the present-day seafloor of the study area, extending from Torrox-Nerja to Motril and from the shelf break, located at a depth ranging from about 100 to > 800 m. The main sources in the area supplying siliciclastic sediments seaward are small rivers like the Guadalfeo River. The physiography is characterized by the presence of morphostructural features such as gradient variations, structural features, mass movements (the Baraza Slide), fluid-dynamic features and channels and canyons. Names of the principal bathymetric features are also displayed

Fig. 4 Map illustrating the gradients of the study area (A) and two bathymetric profiles created with the Fledermaus software package (B-B', C-C'). The location of the map and profiles are shown in (D)

Fig. 5 Map showing the morphology of the Baraza Slide. The slide represents an isolated mass-movement feature in the study area, and is located from 590 to 830 m water depth. Its plan-view morphology is clearly defined by the presence of a well-developed headwall formed by two smaller scars, H1 and H2, and lobes A and B

Fig. 6 Air-gun seismic profile illustrating how the scar plane (H1) extends downslope, going into subsurface sediments and join with the shear plane. See the location in Fig. 2

Fig. 7 Sparker profile illustrating the occurrence of mass-flow features on the slope during the Quaternary. The profile also shows three chronostratigraphic seismic boundaries, represented by reflectors A, B and C, and the seismic units UI, UII and UIII identified as belonging to the Pleistocene sedimentary column. The reflectors were correlated with the TOPAS profiles. Reflector B allows the occurrence of the Baraza Slide to be dated at around 0.69 Ma. See the location in Fig. 2

Fig. 8 Very high resolution seismic profiles obtained by parasound echo-sounder TOPAS, which shows the main sedimentary structure and seismic facies of the Baraza Slide. Reflectors A, B and C and the seismic units UI, UII and UIII are also displayed

Fig. 9 Conceptual schema representing the proposed model for the genesis and development of the Baraza Slide comprising four stages: metastable and failure (A), flowing (B) and sliding (C)

colour figure

Click here to download high resolution image

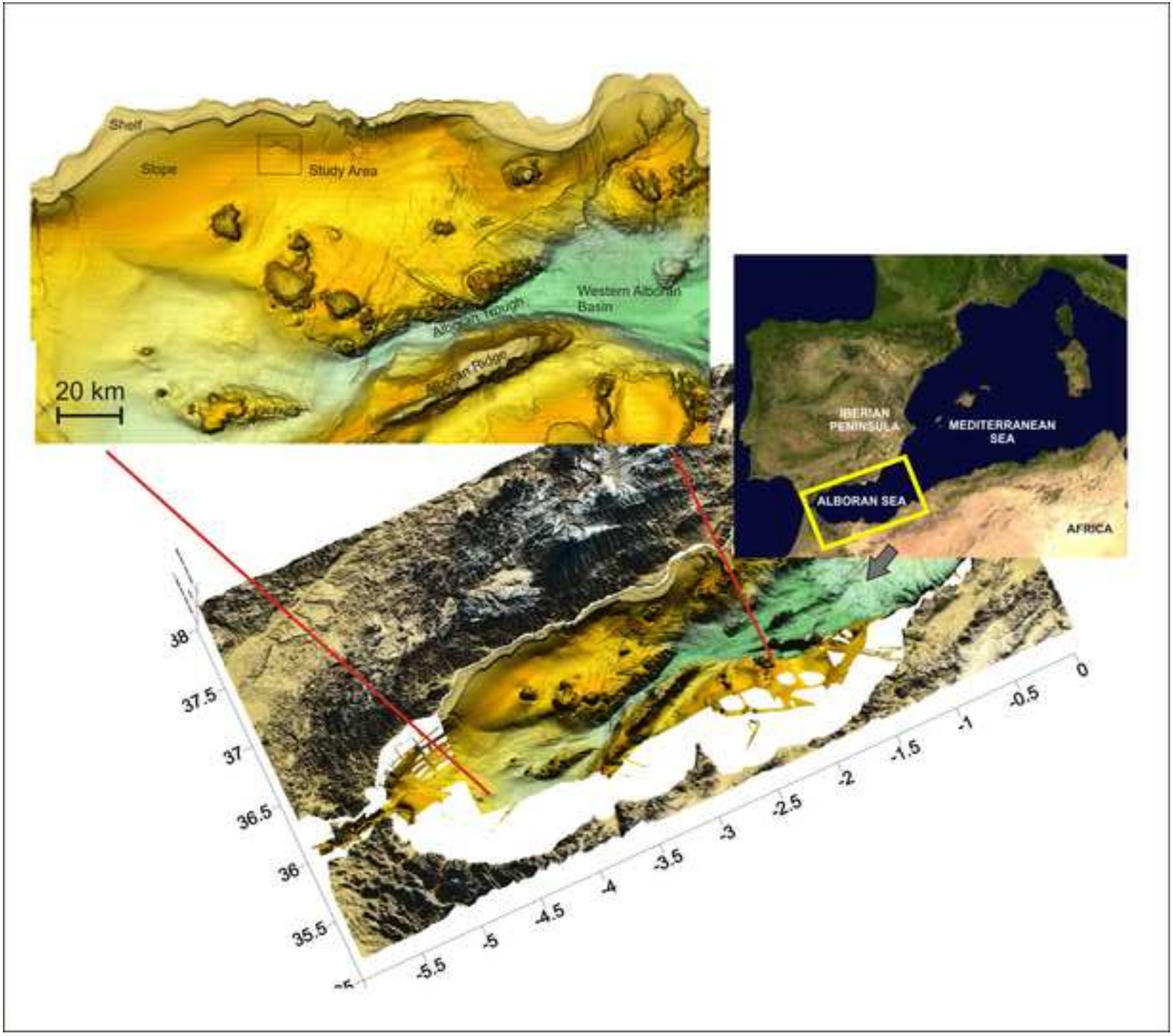

colour figure

Click here to download high resolution image

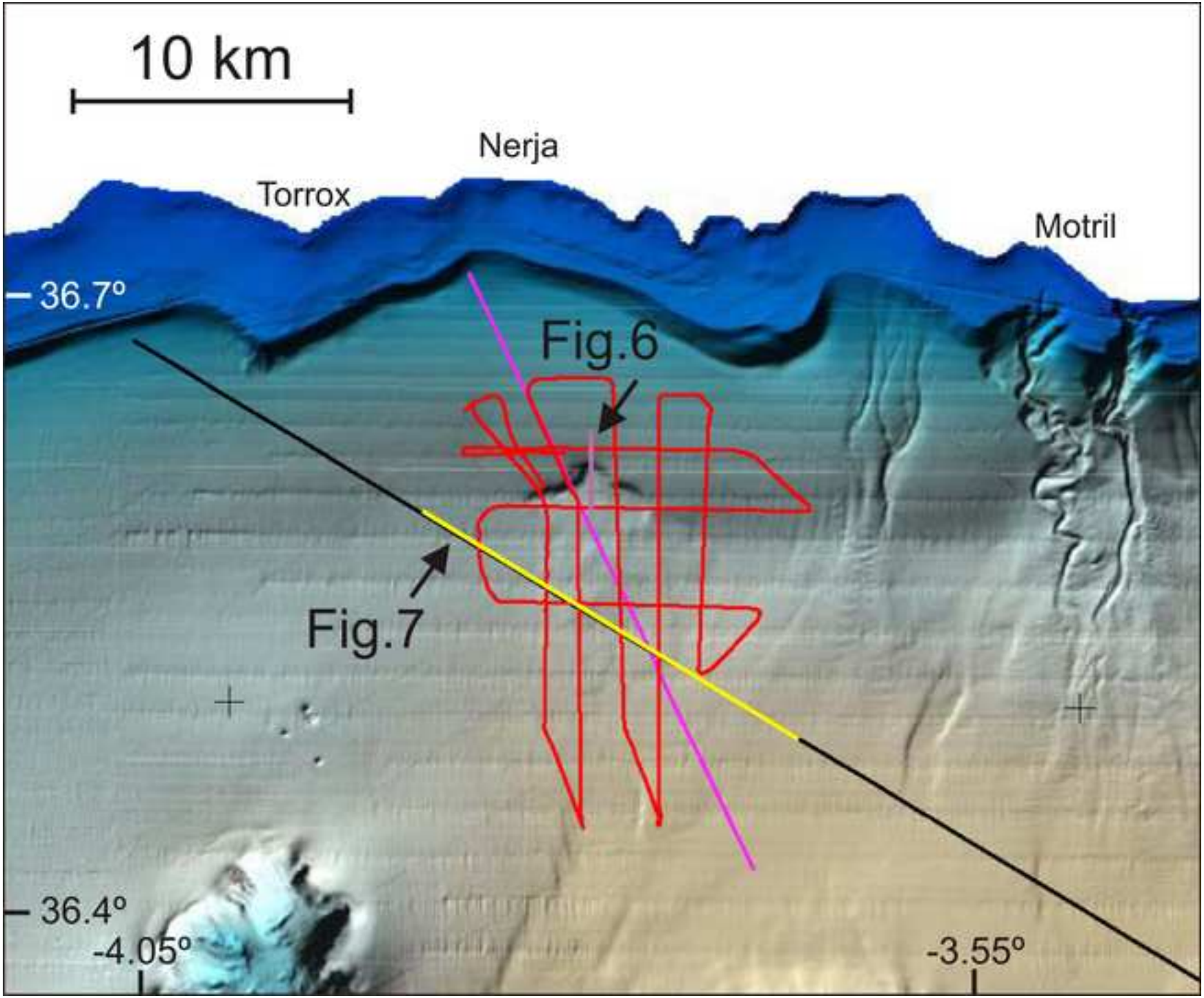

colour figure

Click here to download high resolution image

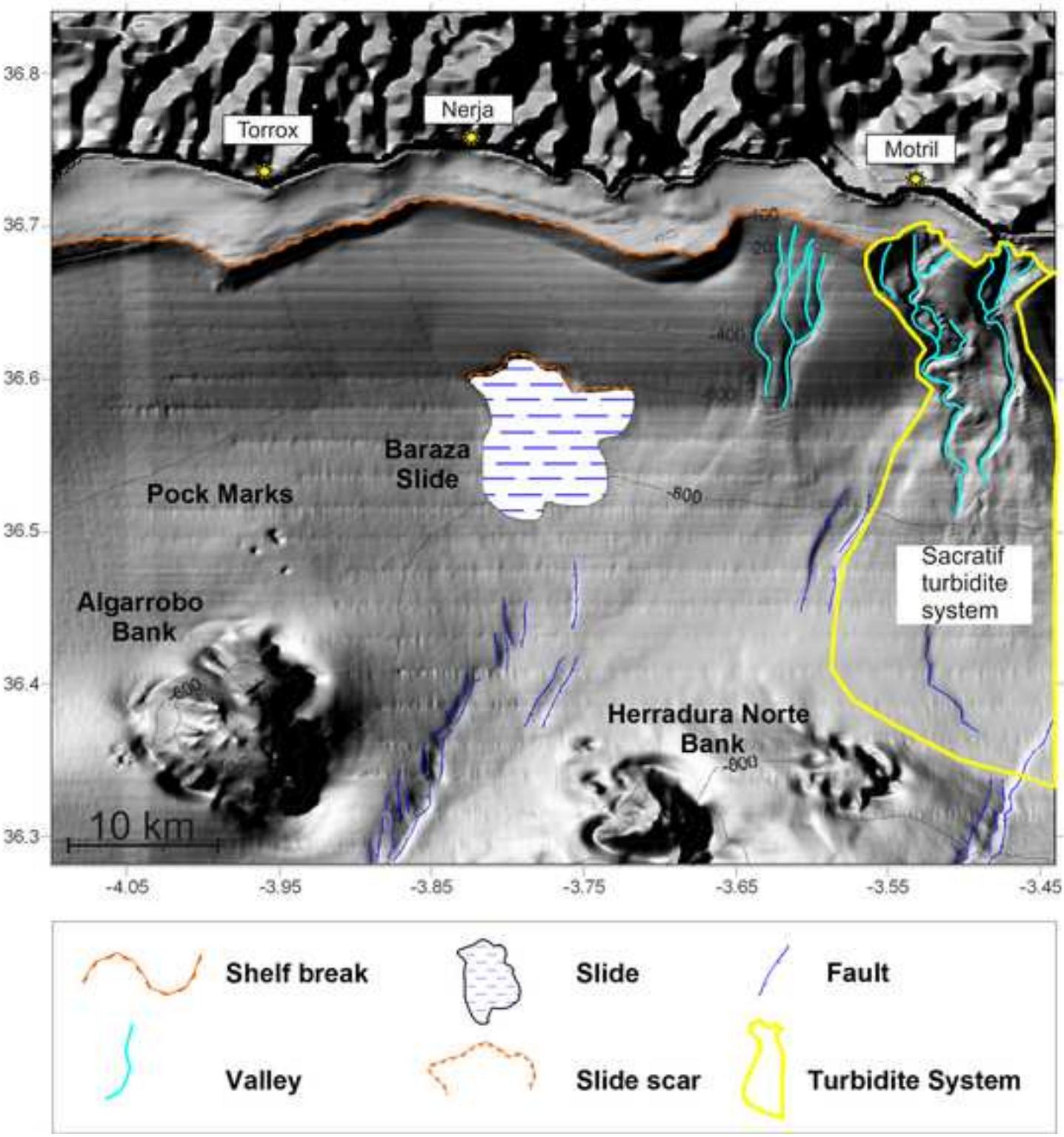

colour figure

Click here to download high resolution image

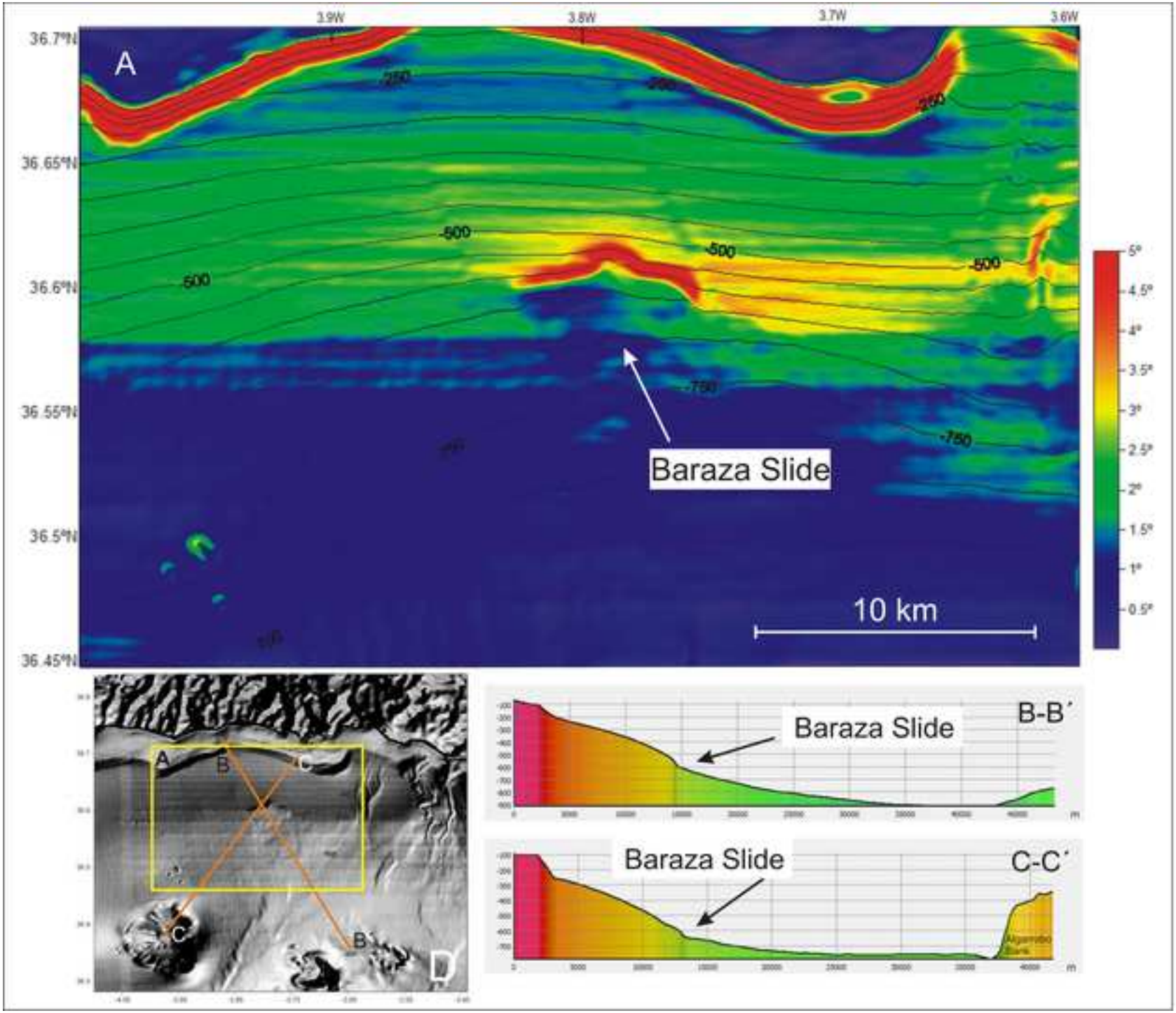

colour figure

Click here to download high resolution image

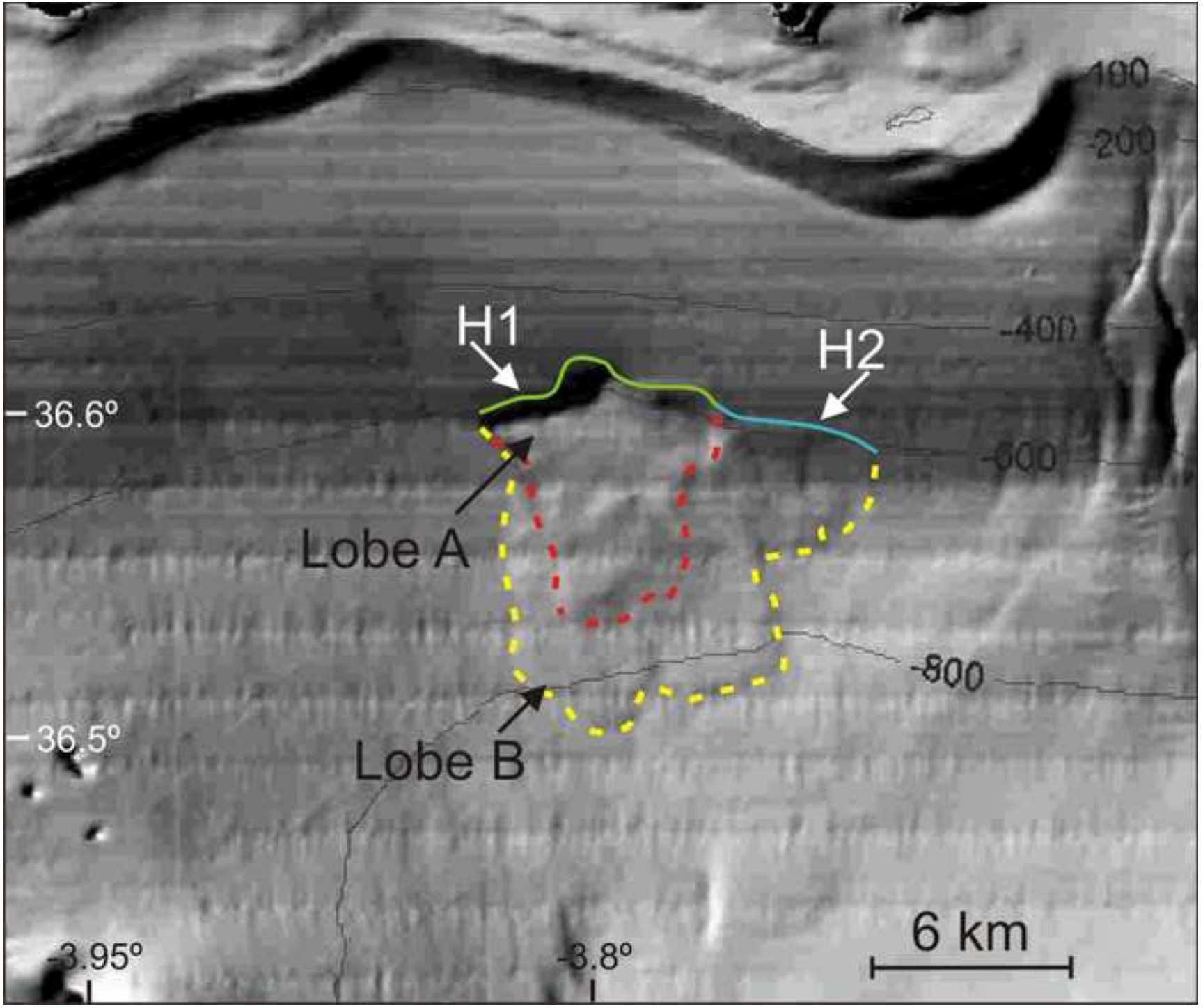

colour figure
Click here to download high resolution image

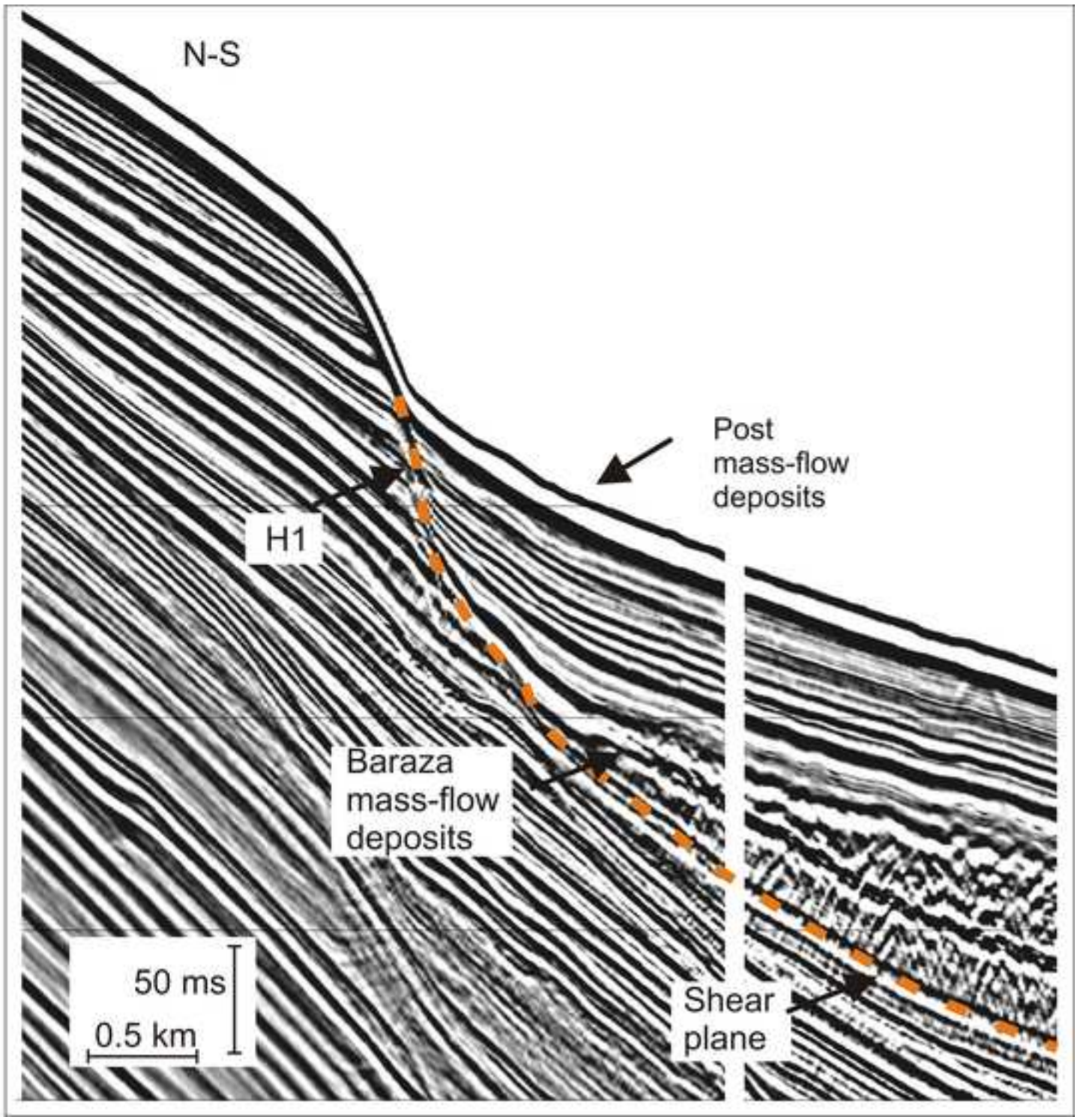

colour figure
Click here to download high resolution image

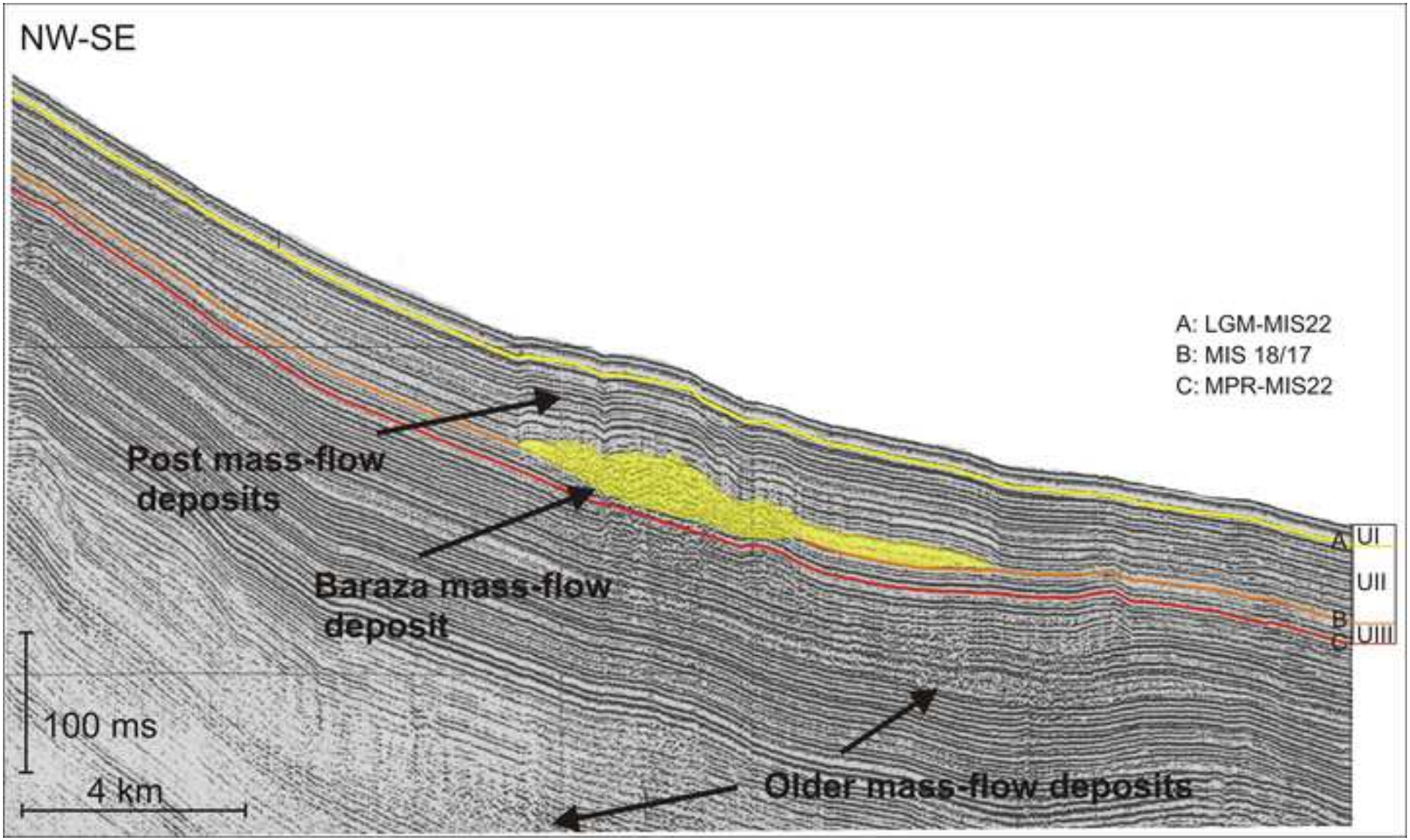

colour figure

Click here to download high resolution image

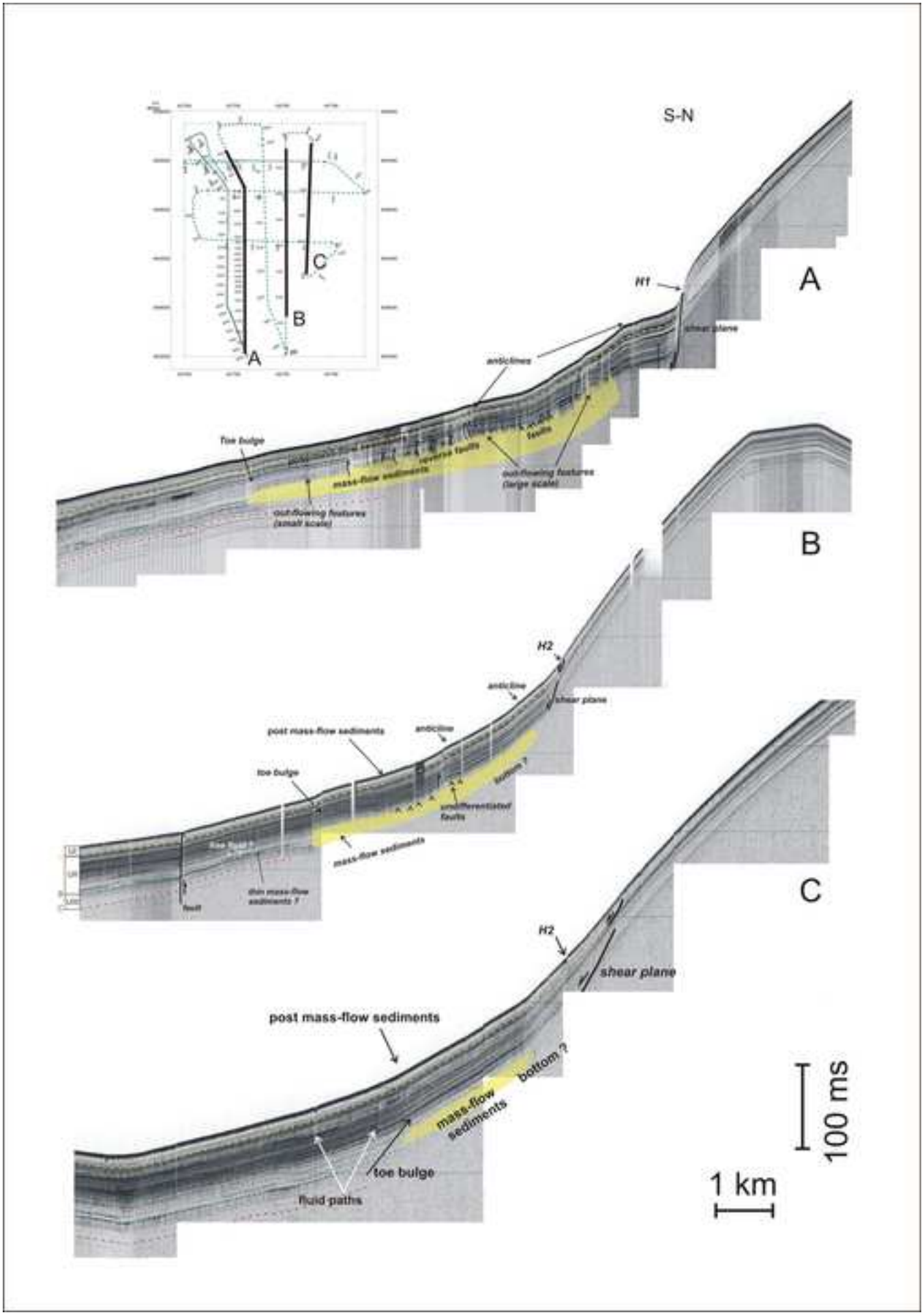

colour figure

Click here to download high resolution image